

Predicting the mechanical properties of spring networks

Doron Grossman^{1,*} and Arezki Boudaoud¹

¹*LadHyX, CNRS, Ecole polytechnique, Institut Polytechnique de Paris, 91128 Palaiseau Cedex, France*

(Dated: December 11, 2023)

The elastic response of mechanical, chemical, and biological systems is often modeled using a discrete arrangement of Hookean springs, either representing finite material elements or even the molecular bonds of a system. However, to date, there is no direct derivation of the relation between a general discrete spring network and its corresponding elastic continuum. Furthermore, understanding the network's mechanical response requires simulations that may be expensive computationally. Here we report a method to derive the exact elastic continuum model of any discrete network of springs, requiring network geometry and topology only. We identify and calculate the so-called "non-affine" displacements. Explicit comparison of our calculations to simulations of different crystalline and disordered configurations, shows we successfully capture the mechanics even of auxetic materials. Our method is valid for residually stressed systems with non-trivial geometries, is easily generalizable to other discrete models, and opens the possibility of a rational design of elastic systems.

Since the 19th century [1, 2], the theory of elasticity has been phenomenological. That is - to date, it has never been derived from first principles as continuum limit, and the elastic properties of a material whose microscopic characteristics are known, could not be computed, in general. Barring some exceptions [3–9] that are limited to classical systems which are neither curved nor exhibit residual stresses, and are not easily generalized. Despite this, it is widely accepted that in essence, linear elasticity may be described using spring-like interactions between constituents (e.g. first order approximation of intermolecular forces around equilibrium). In fact, elasticity is often described using a spring network either for computational or analytical aspects [10, 11] in a plethora of different systems and cases - from modeling the shape of self assembled membranes [12–15], through biological systems [16, 17], to modeling crack propagation [18] and various bio-inspired, and meta materials [19–21]. Typically, calculation of the network's elastic response can only be done via direct simulation of a loading scheme (i.e. simulating a mechanical load and the response to it).

In this paper we directly derive a generalized elastic continuum limit of any triangulated spring network, with arbitrary reference lengths and spring constants, in two and three dimensions, solving an age-long question. The resulting continuum limit depends solely on the network geometry and topology, as expressed by reference lengths, spring constants, and bonds. From this description, any macroscopic elastic quantity can be extracted, such as Poisson's ratio. We demonstrate the strength of this approach, by calculating Poisson's ratios for different test cases, both ordered and disordered, recovering even auxetic behavior. We identify the so-called "non-affine" displacements that are local deformations deviating from the local average deformation, and are responsible of the wide range of responses seen in disordered elastic media. The results are valid for residually stressed elastic systems.

The continuum limit we derive is formulated within the theory of incompatible elasticity,[22] which is a modern formulation of elasticity, that successfully describes residually stressed elastic systems [23–25]. In this formulation, an elastic material is described by a metric \mathbf{g} with elements $g_{\mu\nu}$, which describes actual distances between material elements, and a reference metric $\bar{\mathbf{g}}$ with elements $\bar{g}_{\mu\nu}$ describing ideal distances. The elastic energy then depends on the squared difference of $\mathbf{g} - \bar{\mathbf{g}}$, $E_{el} \propto \|\mathbf{g} - \bar{\mathbf{g}}\|^2$, for some proper choice (yet to be defined) of the norm $\|\cdot\|^2$, through the elastic (four-indexed) tensor \bar{A} (with elements $A^{\mu\nu\alpha\beta}$).

This description, via use of metrics, is very similar in essence and form to the classical description of Hookean springs. It is independent from assumptions about the existence of a rest configuration, which enables the treatment of residual stresses. In the following, we will consider a discrete network of springs and show how such formulation naturally arises. We will then coarse grain the network and will identify the non-affine quantities, and show how they contribute to the elastic continuum energy.

RESULTS

Framework

The theory of incompatible elasticity [22] is the framework to which the results of this paper are anchored to. Within it, the elastic energy is given by:

$$E_{el} = \int A^{\mu\nu\alpha\beta} (g_{\mu\nu} - \bar{g}_{\mu\nu}) (g_{\alpha\beta} - \bar{g}_{\alpha\beta}) dV_{\bar{g}} \quad (1)$$

Where $g_{\mu\nu}$ is the actual metric, describing distances between neighboring material points, $\bar{g}_{\mu\nu}$ is the reference metric, describing ideal distances. $dV_{\bar{g}} = \sqrt{\bar{g}} d^M x$ is the volume element in M dimensions, $\bar{g} = \det \bar{\mathbf{g}}$. $A^{\mu\nu\alpha\beta}$ is the elastic tensor. Einstein's summation is assumed for repeating upper and lower Greek indices. Greek indices refer to coordinates within the volume of the n dimensional manifold.

In an isotropic material, $A^{\mu\nu\alpha\beta} = \frac{Y}{16(1-\nu^2)} [\frac{1}{2}(1-\nu)(\bar{g}^{\mu\alpha}\bar{g}^{\nu\beta} + \bar{g}^{\nu\alpha}\bar{g}^{\mu\beta}) + \nu\bar{g}^{\mu\nu}\bar{g}^{\alpha\beta}]$, where $\bar{g}^{\mu\nu}$ is the inverse reference metric, Y is Young's modulus, setting the rigidity scale of the system, and ν is Poisson's ratio, describing the amount a material contracts in one axis, when the other is stretched (negative values indicate expansion). In non isotropic materials Poisson's ratio is orientation dependent, and the expression of $A^{\mu\nu\alpha\beta}$ will typically depend on additional terms.

The elastic stress is given by the variation $\sigma^{\mu\nu} = \frac{\delta E_{el}}{\delta g_{\mu\nu}}$, and the material satisfies the usual force balance equation:

$$\bar{\nabla}_{\mu}\sigma^{\mu\nu} + \sigma^{\mu\alpha}(\Gamma_{\mu\alpha}^{\nu} - \bar{\Gamma}_{\mu\alpha}^{\nu}) = f_{ext}^{\nu} \quad (2)$$

where f_{ext}^{ν} are the external forces acting on the systems, and $\sigma^{\mu\nu} = \frac{\delta E_{el}}{\delta g_{\mu\nu}}$ is the elastic stress, $\bar{\nabla}_{\mu}$ is the covariant derivative with respect to $\bar{g}_{\mu\nu}$ and $\Gamma_{\beta\gamma}^{\alpha}, \bar{\Gamma}_{\beta\gamma}^{\alpha}$ are the christoffel symbols associated with the metrics $g_{\mu\nu}$ and $\bar{g}_{\mu\nu}$ respectively.

Analytical Derivation

We begin by considering a triangulated mesh of springs, each with reference length ℓ_e , spring constant k_e and an actual length l_e , where the index e enumerates the springs. The elastic energy of the systems is exactly given by

$$E_{el} = \sum_e \frac{1}{2} k_e (l_e - \ell_e)^2. \quad (3)$$

A triangulated network is easily divided into sum of specific simplexes (cells). In three dimensions these are tetrahedrons, and in two dimensions these are simple triangles

$$E_{el} = \frac{1}{2} \sum_s \sum_{e \in s} \frac{1}{2} k_e (l_e - \ell_e)^2. \quad (4)$$

Here, the index s enumerates simplexes, $e \in s$ means summation over all the springs associated with the simplex s . When left to relax, the network assumes some configuration (not necessarily unique) $\{\vec{f}_v\}$ in \mathbb{R}^m for every vertex v . By Setting coordinates x_v^{μ} to each vertex v (μ is the coordinate component), given actual lengths $\{l_e\}$, we may uniquely define a "local metric" $g_{\mu\nu}^{(s)}$ associated with a cell s , so that

$$l_e^2 = g_{\mu\nu}^{(s)} \Delta x_e^{\mu} \Delta x_e^{\nu} \quad \forall e \in s. \quad (5)$$

Where $\Delta x_{(1,2)}^{\mu} = x_2^{\mu} - x_1^{\mu}$ is the "coordinate difference" of the edge $e = (1,2)$ connecting vertexes 1 and 2. (5) is not an approximation, rather it is an exact definition of the local quantity $g_{\mu\nu}^{(s)}$, over the whole simplex.

Hence, a given simplex uniquely defines a local metric, $g_{\mu\nu}^{(s)}$, associated to it. A physical systems is constrained such that any two local metrics $\mathbf{g}^{(i)}$ and $\mathbf{g}^{(j)}$ with a shared edge Δx_e , agree on its length- $l_e[\mathbf{g}^{(i)}] = l_e[\mathbf{g}^{(j)}]$, where $l_e[\mathbf{g}]$ is

the edge's length, as measured using the metric \mathbf{g} . We can now rewrite the energy -

$$E_{el} = \frac{1}{4} \sum_s \sum_{e \in s} k_e \left(\sqrt{g^{(s)}_{\mu\nu} \Delta x_e^\mu \Delta x_e^\nu} - \ell_e \right)^2. \quad (6)$$

In order to advance, we introduce three assumption. First we assume that the reference lengths $\{\ell_e\}$ are compatible, so that a single simplex can assume the shape described by the lengths ℓ_e . This means that the reference lengths locally define a reference metric $\bar{g}_{\mu\nu}^{(s)}$. Under these assumptions we can write $\ell_e = \sqrt{\bar{g}_{\mu\nu}^{(s)} \Delta x_e^\mu \Delta x_e^\nu}$.

Second, we assume that in an equilibrium configuration (again, not necessarily unique), deviations of actual lengths from the reference lengths are small.

$$l_e - \ell_e = \frac{l_e^2 - \ell_e^2}{l_e + \ell_e} \simeq \frac{1}{2\ell_e} (l_e^2 - \ell_e^2) + \dots \quad (7)$$

\dots marks higher order terms of $l_e^2 - \ell_e^2$. Thus

$$E_{el} = \sum_s \sum_{e \in s} \frac{k_e}{16\ell_e^2} \left(g_{\mu\nu}^{(s)} \Delta x_e^\mu \Delta x_e^\nu - \bar{g}_{\mu\nu}^{(s)} \Delta x_e^\mu \Delta x_e^\nu \right)^2 + \dots \quad (8)$$

We expand the energy:

$$E_{el} = \sum_s \left(g_{\mu\nu}^{(s)} - \bar{g}_{\mu\nu}^{(s)} \right) \left(g_{\alpha\beta}^{(s)} - \bar{g}_{\alpha\beta}^{(s)} \right) \sum_{e \in s} \frac{k_e \Delta x_e^\mu \Delta x_e^\nu \Delta x_e^\alpha \Delta x_e^\beta}{16\ell_e^2}. \quad (9)$$

Marking the local elastic tensor

$$A_{(s)}^{\mu\nu\alpha\beta} = \sum_{e \in s} \frac{k_e \Delta x_e^\mu \Delta x_e^\nu \Delta x_e^\alpha \Delta x_e^\beta}{16\ell_e^2}, \quad (10)$$

we write -

$$E_{el} = \sum_s A_{(s)}^{\mu\nu\alpha\beta} \left(g_{\mu\nu}^{(s)} - \bar{g}_{\mu\nu}^{(s)} \right) \left(g_{\alpha\beta}^{(s)} - \bar{g}_{\alpha\beta}^{(s)} \right) \quad (11)$$

This equation is very similar to (1), and may be considered as a discrete version of that equation.

The last assumption introduced, is that \bar{g}_s varies slowly on some large enough region. Without this assumption the continuum limit cannot hold (though an effective continuum may be derived, in principle).

Defining an average metric, $g_{\mu\nu}$, on some neighborhood, we may expand $g_{\mu\nu}^{(s)} = g_{\mu\nu} + \delta g_{\mu\nu}^{(s)}$. Formally, $\delta g_{\mu\nu}^{(s)}$ describe the "non-affine" deformations. The energy then reads -

$$E_{el} = \sum_{\Omega} \left(\sum_{s \in \Omega} A_{(s)}^{\mu\nu\alpha\beta} \Delta g_{\mu\nu} \Delta g_{\alpha\beta} + \sum_{s \in \Omega} A_{(s)}^{\mu\nu\alpha\beta} \Delta g_{\mu\nu} \delta g_{\alpha\beta}^{(s)} + \sum_{s \in \Omega} A_{(s)}^{\mu\nu\alpha\beta} \delta g_{\mu\nu} \Delta g_{\alpha\beta}^{(s)} + \sum_{s \in \Omega} A_{(s)}^{\mu\nu\alpha\beta} \delta g_{\mu\nu}^{(s)} \delta g_{\alpha\beta}^{(s)} \right), \quad (12)$$

where $\Delta g_{\mu\nu} = g_{\mu\nu} - \bar{g}_{\mu\nu}$, and \sum_{Ω} is the sum over all the neighborhoods in which \mathbf{g} and $\bar{\mathbf{g}}$ may be regarded as constant. Since, under our assumptions, if $g_{\mu\nu} = \bar{g}_{\mu\nu}$, $\delta g_{\mu\nu}^{(s)} = 0 \forall s$, then for small deviations from $\bar{g}_{\mu\nu}$, $\delta g_{\mu\nu}^{(s)} = W_{(s)\mu\nu}^{\alpha\beta} \Delta g_{\alpha\beta}$. While mathematically different, we identify the proportion tensors $W_{(s)\mu\nu}^{\alpha\beta}$, with the "non affine" deformations of each simplex, which are yet unknown.

The elastic energy E_{el}^{Ω} within a single neighborhood ($E_{el} = \sum_{\Omega} E_{el}^{\Omega}$) then reads

$$E_{el}^{\Omega} = \sum_s \left(A_{(s)}^{\mu\nu\alpha\beta} + A_{(s)}^{\mu\nu\rho\sigma} W_{(s)\rho\sigma}^{\alpha\beta} + A_{(s)}^{\alpha\beta\rho\sigma} W_{(s)\rho\sigma}^{\mu\nu} + A_{(s)}^{\tau\lambda\rho\sigma} W_{(s)\rho\sigma}^{\alpha\beta} W_{(s)\tau\lambda}^{\mu\nu} \right) \Delta g_{\mu\nu} \Delta g_{\alpha\beta} \quad (13)$$

$$+ \chi^{\alpha\beta} \sum_s W_{(s)\alpha\beta}^{\mu\nu} \Delta g_{\mu\nu}$$

The second line is a Lagrange term forcing the requirement that $\sum_s \delta g_{(s)\mu\nu} = 0$. We note, that as $g_{\mu\nu}$ is an average

metric, $\sum_s \delta g_{\mu\nu}^{(s)} = 0$. This translates to $\sum_s W_{(s)\mu\nu}^{\alpha\beta} = 0$. Marking n the number of simplexes in the neighborhood Ω , and the averages:

$$A^{\mu\nu\alpha\beta} = \frac{1}{n} \sum_s A_{(s)}^{\mu\nu\alpha\beta} \quad (14)$$

$$\tilde{A}^{\mu\nu\alpha\beta} = \frac{1}{n} \sum_s \left(A_{(s)}^{\mu\nu\alpha\beta} + A_{(s)}^{\mu\nu\rho\sigma} W_{(s)\rho\sigma}^{\alpha\beta} + A_{(s)}^{\alpha\beta\rho\sigma} W_{(s)\rho\sigma}^{\mu\nu} + A_{(s)}^{\tau\lambda\rho\sigma} W_{(s)\rho\sigma}^{\alpha\beta} W_{(s)\tau\lambda}^{\mu\nu} \right) \quad (15)$$

$$\delta A_{(s)}^{\mu\nu\alpha\beta} = A_{(s)}^{\mu\nu\alpha\beta} - A^{\mu\nu\alpha\beta}, \quad (16)$$

we may find $W_{(s)\mu\nu}^{\alpha\beta}$ for a finite strain by solving the coupled set of equations

$$\begin{aligned} \bar{\nabla}_\mu \sigma^{\mu\nu} + \sigma^{\mu\alpha} (\Gamma_{\mu\alpha}^\nu - \bar{\Gamma}_{\mu\alpha}^\nu) &= f_{ext}^\nu \\ \left(A_{(s)}^{\mu\nu\alpha\beta} + A_{(s)}^{\lambda\tau\alpha\beta} W_{(s)\lambda\tau}^{\mu\nu} \right) \Delta g_{\mu\nu} + \frac{1}{2} \chi^{\alpha\beta} &= 0 \end{aligned} \quad (17)$$

The first line is actually the elastic equation(2). At this point it is enough to note that $\sigma^{\mu\nu} = \frac{\delta E_{el}}{\delta g_{\mu\nu}}$, where E_{el} is given by eq. (13), that $\Gamma_{\beta\gamma}^\alpha$ and $\bar{\Gamma}_{\beta\gamma}^\alpha$ are the Christoffel symbols associates with the metrics \mathbf{g} and $\bar{\mathbf{g}}$, and $\bar{\nabla}_\mu$ is the covariant derivative associated with the metric $\bar{\mathbf{g}}$. Marking $\langle A_{(s)} W_{(s)} \rangle^{\mu\nu\alpha\beta} = \frac{1}{n} \sum_s A_{(s)}^{\lambda\tau\alpha\beta} W_{(s)\lambda\tau}^{\mu\nu}$, and using $\langle A_{(s)} W_{(s)} \rangle^{\mu\nu\alpha\beta} = \langle \delta A_{(s)} W_{(s)} \rangle^{\mu\nu\alpha\beta}$, we may rewrite the second line of (17), after a little algebra

$$\delta A_{(s)}^{\mu\nu\alpha\beta} + A_{(s)}^{\lambda\tau\alpha\beta} W_{(s)\lambda\tau}^{\mu\nu} - \langle \delta A_{(s)} W_{(s)} \rangle^{\mu\nu\alpha\beta} = 0. \quad (18)$$

This is a linear equation for the non-affine deformation terms, W . It is solved by mapping the tensor components and indexes unto a multi - index notation and using the symmetries of the tensors (in two dimensions $W_{(s)\mu\nu}^{\alpha\beta}$ has only 9 independent entries, while in three dimension it has 36)

$$\delta A_S + \sum_{S'} (A_{SS'} - B_{SS'}) W_{S'} = 0 \quad (19)$$

Where δA_S , $A_{SS'}$ and $B_{SS'}$ are reorganizations of the elements of $\{A_s^{\mu\nu\alpha\beta}\}$ and $\{\delta A_s^{\mu\nu\alpha\beta}\}$ into matrices compatible with the new multi index (see appendix A). The solution -

$$W_S = - \sum_{S'} [A - B]^{-1}_{SS'} \delta A_{S'}. \quad (20)$$

We may now write the elastic energy -

$$E_{el} = \sum_\Omega n \tilde{A}^{\mu\nu\alpha\beta} (g_{\mu\nu} - \bar{g}_{\mu\nu}) (g_{\alpha\beta} - \bar{g}_{\alpha\beta}). \quad (21)$$

This equation is essentially already coarse grained -

$$\begin{aligned} E_{el} &= \sum_\Omega n \tilde{A}^{\mu\nu\alpha\beta} (g_{\mu\nu} - \bar{g}_{\mu\nu}) (g_{\alpha\beta} - \bar{g}_{\alpha\beta}) \frac{V_\Omega}{V_\Omega} = \sum_\Omega \rho_\Omega \tilde{A}^{\mu\nu\alpha\beta} (g_{\mu\nu} - \bar{g}_{\mu\nu}) (g_{\alpha\beta} - \bar{g}_{\alpha\beta}) \int_\Omega dV_{\bar{\mathbf{g}}} \\ &= \int \tilde{A}^{\mu\nu\alpha\beta} (g_{\mu\nu} - \bar{g}_{\mu\nu}) (g_{\alpha\beta} - \bar{g}_{\alpha\beta}) dV_{\bar{\mathbf{g}}} \end{aligned} \quad (22)$$

where V_Ω is the volume of the neighborhood Ω , $\rho_\Omega = n/V_\Omega$ is the local density (which we absorb into the definition of $\tilde{A}^{\mu\nu\alpha\beta}$), $\int_\Omega dV_{\bar{\mathbf{g}}}$ is an integral over the region Ω and we use the fact the $\sum_\Omega \int_\Omega dV_{\bar{\mathbf{g}}} = \int dV_{\bar{\mathbf{g}}}$ over all the network.

Eqs. (22), and (20) form the central result of this work. Together with the definitions of $A^{\mu\nu\alpha\beta}$, $\tilde{A}_s^{\mu\nu\alpha\beta}$, $W_{(s)\lambda\tau}^{\mu\nu}$, they fully describe the response of the network and offer a novel way of computing it directly from the network geometry, without the need to consider any specific load. Under this view the metrics \mathbf{g} is the actual, coarse grained, metric of the system, $\bar{\mathbf{g}}$ describes the reference geometry of the system, and $\tilde{A}^{\mu\nu\alpha\beta}$ is the coarse grained elastic tensor, governing the mechanical response (as opposed to the local or "bare" term $A_{(s)}^{\mu\nu\alpha\beta}$). $W_{(s)\alpha\beta}^{\mu\nu}$ describe the non-affine

displacements.

Comparison to simulation

Results were tested numerically by comparing the expected Poisson's ratio using the above scheme, to that of simulated two dimensional triangulated spring networks. In general, we find a very good agreement between theory and simulation, the details of which are described in the methods section. We considered three cases - ordered, foam-like, and honeycomb networks.

Ordered networks

In the ordered case we simulated a triangular lattice of varying unit cells' shapes, and computed the angle dependence Poisson's ratio. In this case all of the non-affine tensors $W_{(s)\mu\nu}^{\alpha\beta} = 0$ identically vanish, leading to a simple calculation using eq.(10) (detailed analysis in appendix C). In Figure 1, we see comparison of the analytical solution, and the numerical estimation. Insets show the lattice structure.

Foam-like

Following [20] we simulate a random, foam-like, network, exhibiting an auxetic behavior at certain parameter range. Network is produced by deforming each vertex position of a regular triangular lattice, in random direction by a fixed amount $0 < \eta < 0.5$. Calculation was done several times to average the results. Our results are consistent with the those in [20] - ν decreases as a function of η reaching $\nu = 0$ at $\eta \simeq 0.46$ and reaching $\nu = -0.1$ when $\eta \rightarrow 0.5$. In the left side fig. 2 we compare the simulation (discrete triangles) and the semi-analytical computation described in this paper.

Additionally, we can directly visualize the network response. By calculating $\delta g_{\mu\nu} = W_{\mu\nu}^{\alpha\beta} \Delta g_{\alpha\beta}$, we may find the response of each triangulated region. An example of the visualization may be found in inset of right image in Fig. 2. Most notably, it is clear that the change in Poisson's ratio is related to the response of high aspect-ratio triangles that occur randomly via the process described. In these triangles one of the edges is exceptionally short, and given the uniform spring constant distribution used, this translates to lower local rigidity value which intuitively means stronger response. To quantify the total response of a network, we calculated the eigenvalues of the response coefficients $\frac{\delta g_{\mu\nu}}{\epsilon}$ of each triangle, then averaged the determinant ($D = \det \frac{\delta g_{\mu\nu}}{\epsilon}$) and the square of the trace ($T^2 = \left(\text{Tr} \frac{\delta g_{\mu\nu}}{\epsilon} \right)^2$) (as the average of the trace by definition vanishes over the whole network). These are plotted on the right side of fig. 2.

Hexagonal (honeycomb) network

We consider a honeycomb network, in which the basic hexagonal unit can vary between regular and a re-entrant hexagon, continuously with a diameter (distance between two opposing vertexes) of 2ℓ $0 < \ell < 1$. (see inset in fig. 3). In such a case, Poisson's ratio is analytically given [26]

$$\nu(\ell) = -\frac{(2-4\ell)(\ell+1/2)}{3+4\ell-4\ell^2} \quad (23)$$

In order to calculate the elastic response, we use a triangularized hexagon, with a vertex at the center, and set the spring constant of the radial springs connecting the center with each corner of the hexagon to a very small value (1/1000'th of the peripheral springs). Without this, the original formulation become singular when the spring constant vanishes completely. Results are shown in fig. 3 with a very high degree of agreement between the analytical result and our formulation, despite the use of a large difference between springs constants, strengthening our approach.

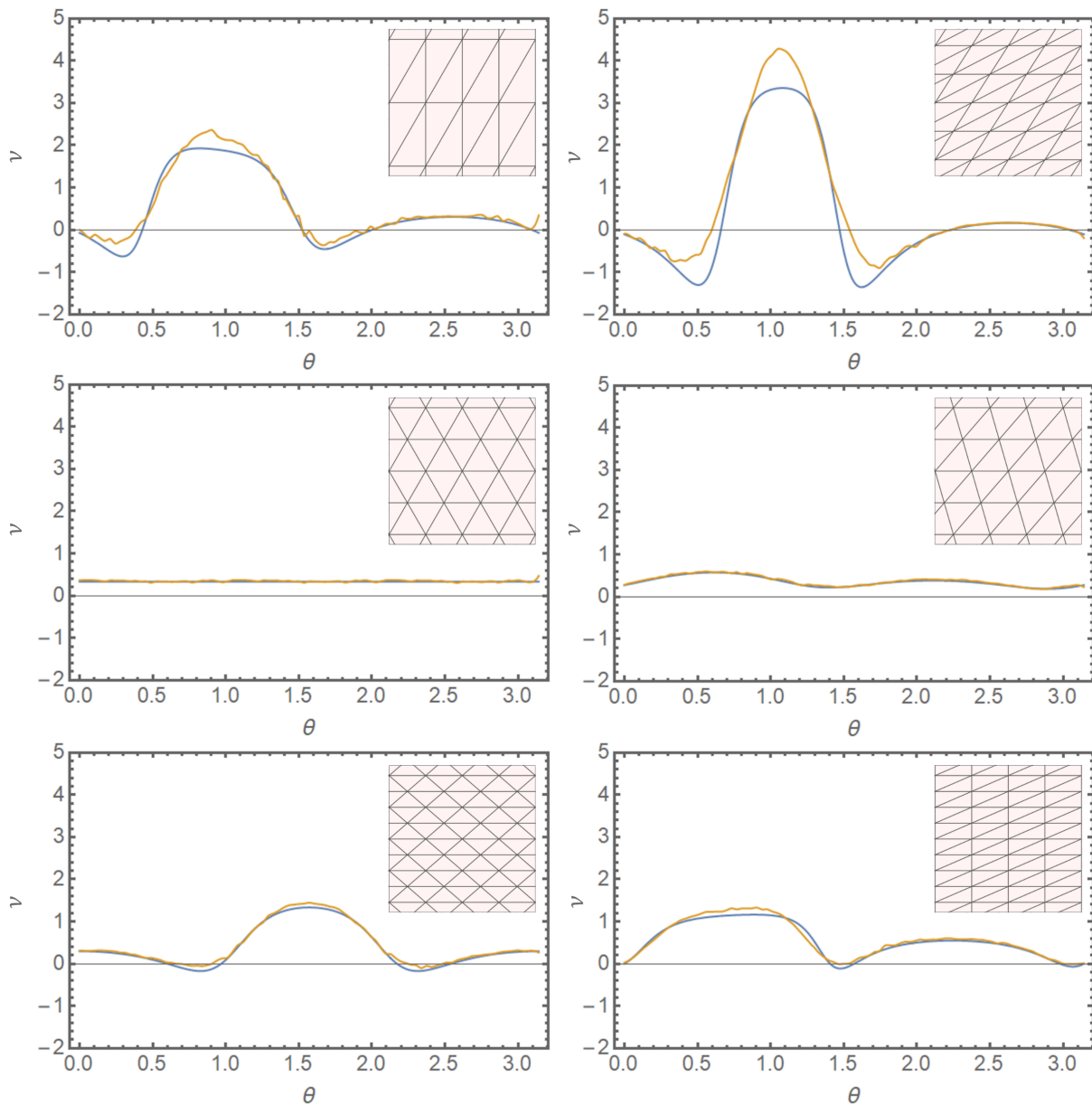


FIG. 1: Ordered networks. Simulation (yellow) vs analytical estimation (blue) of Poisson's ratio as a function of the angle depending on different shape parameters (ϕ, ψ) . Beginning in the middle row, left image, and advancing clockwise: $(\phi = 1, \psi = 1)$, $(2, 2)$, $(3, 0.9)$, $(1.5, 1)$, $(2, 0.5)$, $(1, 0.5)$. Insets- the spring network shape (up to rotations)

CONCLUSIONS

In this work we give, to our knowledge, the first analytical derivation of the effective, coarse grained, elastic description of a general spring network. Comparison of computational results stemming from this derivation to known/numerical results shows a high degree of agreement. Additionally, we identified and quantified the "non-affine" deformations, and have shown how they affect the resulting continuum elastic model, and related them to network structure. In systems such as granular media, these quantities play a role in local stress release by means of plastic deformations [27].

While derived over a spring-network, the results' derivation shown is relevant to many fields and systems in two ways. First the interaction between elements is almost always approximated as that of a simple spring, especially at small deformation. This is true for mechanical systems such as meta materials [19–21] and coarse grained mechanical models[18], chemical systems such as self assemblies [12–15], and many biological systems as well [16, 17]. As such,

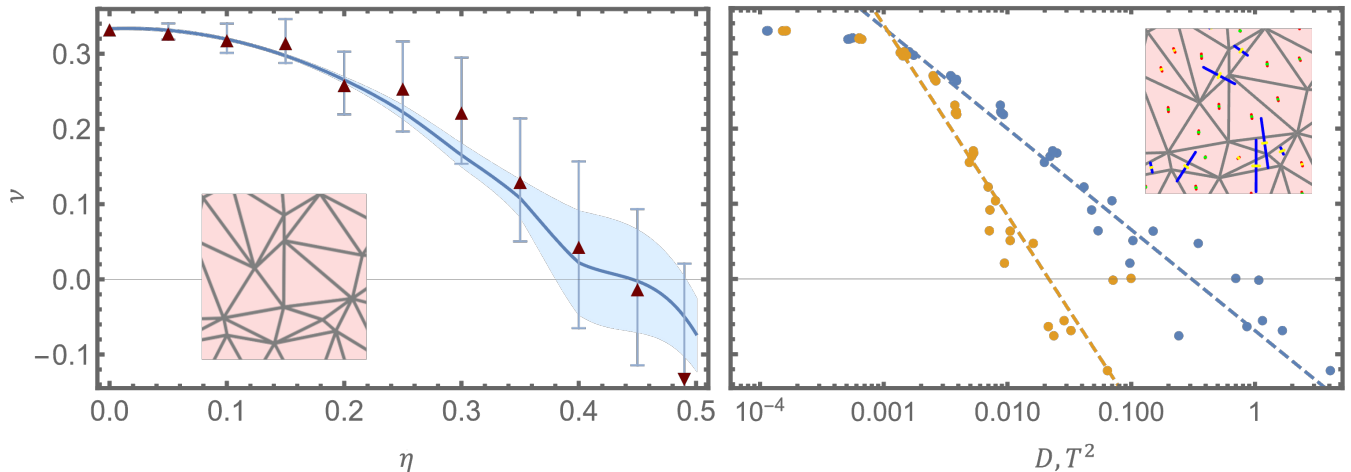


FIG. 2: Random foam-like networks. Left - Comparison between theoretical calculation (solid line) and numerical simulation (triangles). Solid line represents the average of 7 different realizations of about 150 vertexes each (shaded region is typical deviation). Numerical simulations were done over 10 realizations of 676 vertexes each, error bars mark the deviations. Note that the last triangle is pointing down, indicating the average is beyond plot boundaries.

Inset- an example of a $\eta = 0.3$ realization. Right - Relation between Poisson's ratio, to the response averages D (yellow) and T^2 (blue) (see text for description) quantifying the network response. Points are the calculated results for different realizations, dashed lines - trend indicators. Inset - same inset as in Left, this time with principal components of $\frac{\delta g_{\mu\nu}}{\epsilon}$. Blue and red - elongation or contraction of major principal direction (respectively). Yellow and green - out-of-phase or in-phase response of minor principal direction relative to the major direction. Size of lines - relative size of principal response coefficients.

the resulting theory, as is, is relevant to engineers, physicists, chemists, and biologist, and opens the possibility of rational design of materials.

Second, the coarse graining process described here can be generalized to other, more complicated interactions, and is not limited to point masses connected by linear springs. Nonlinearities can be addressed by using higher orders terms (shape - related nonlinearities are actually addressed by the usage of a metric description). Formulated correctly it could apply to complex molecules, cell-cell interactions, and to polymer-networks. Activity may be involved in it as well.

Finally, the introduction of the new, W , quantities invites further investigation as to the nature of the solutions of eq.(20), both analytically, and numerically. It is known, for example, that the non-affine deformations have a characteristic scale [27], this formulation may allow further insight into their scale dependence. Other usages route would involve intelligent design - relating the required mechanical behavior to the non-affine deformations, and from that to the network structure.

METHODS

We used our assumptions that $\bar{\mathbf{g}}$ is well defined on a large enough region to limit our numerical and analytical solution for the case $\bar{g}_{\mu\nu} = \delta_{\mu\nu}$, as we can always work in a locally flat frame. This condition is sufficient as we want to isolate the effects of the non-trivial structure of the network itself, not the whole (non uniform) mechanical response of a complex, possibly residually stressed structure. We compared the results of 3 test cases, ordered (non isotropic), foam like (following procedure in [20]), and a honeycomb, despite the latter being strictly - non triangulated. The latter can be calculated analytically, rather than simulated.

In parallel to simulation, for every network architecture we calculated $\tilde{A}^{\mu\nu\alpha\beta}$ and using it, we calculated the response to a hypothetical small strain ϵ by setting $g_{yy} = 1 + \epsilon$. Using the elastic equation (17), and working in a geometric mean-field approximation, we solved the other terms g_{xx} and g_{xy} and calculate Poisson's ratio $\nu = -\frac{g_{xx}-1}{\epsilon}$ (see appendix B for details).

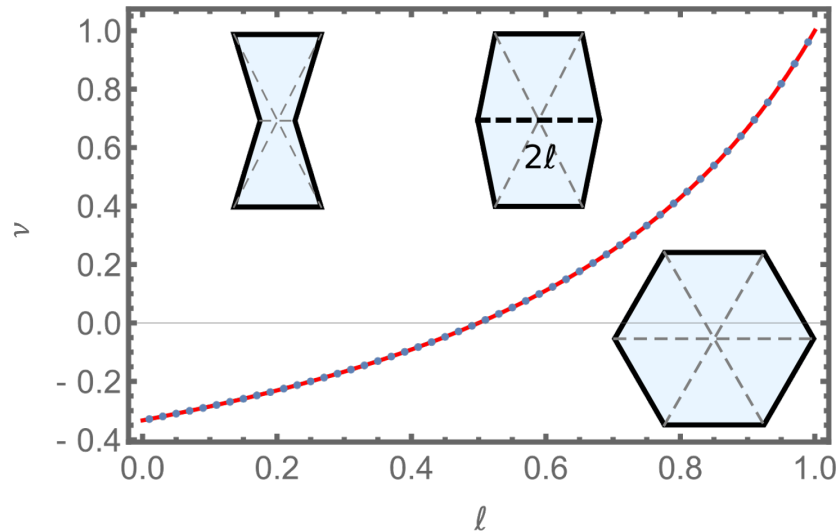


FIG. 3: Hexagonal networks. Theoretical (solid line) and computational (points) results for a honeycomb made out of uniform hexagons with diameter 2ℓ . To avoid singular expressions, each hexagon was divided to triangles (as indicated by dashed lines). Such that the added edges had negligible, but finite, rigidity ($k_{dashed} = 10^{-3}k_{solid}$), insets (from left to right - re-entrant hexagon, general hexagon, regular hexagon)

Simulation

The simulation was created for the purpose of this research. In each run we simulated a strip with length to width ratio of 4:1. A total of about $13 \times 13 \times 4 = 676$ vertices, corresponding to about 1000 edges, depending on the exact details of each simulation.

When creating a lattice, vertices were positioned using the base vectors -

$$\begin{aligned} v_1 &= (1, 0) \\ v_2 &= \left(\phi \frac{1}{2}, \psi \frac{\sqrt{3}}{2} \right) \end{aligned} \quad (24)$$

where $0 < \phi, \psi$ are the shear and elongation parameters, respectively, and are used to control the shape of the triangles. $\psi = \phi = 1$ corresponds to an equilateral triangle, and any $\phi = 1$ is an isosceles triangle. The strip was created by keeping all vertices whose coordinates satisfy $0 \leq x \leq 13$ and $0 \leq y \leq 52$ ("trimming"). Different orientations lattices were created by rotating the base vectors before trimming, so that the strip orientation remains constant, but the orientation of triangles relative to it changes.

The set of vertices was then used to create the list of edges via triangulation, and extracting the list of neighbors. The energy of each edge was directly calculated from the positions of its vertices, using a simple spring energy. In the simulation, the positions of the top and bottom vertices is held constant and all other vertices are allowed to move in order to minimize the total energy.

The two vertices initially closest to $x = 0, y = 26$ and $x = 13, y = 26$ were identified to measure the strain between them $\delta = \frac{\Delta x_{final}}{\Delta x_{initial}}$, where Δx_{final} is the final x -coordinate difference between the two vertices, and $\Delta x_{initial}$ is the initial difference. After setting the top vertices at $y = 52(1 + \epsilon)$ ($\epsilon = 0.01$), and letting the system to relax elastically, Poisson's ratio was calculated via $\nu = -\delta/\epsilon$. And averaged over several simulations, if required (in the more stochastic simulations).

Simulating the foam-like structure, is stochastic in essence. We used the same initialization process, with the following differences. After generating a triangular lattice strip with $\phi = \psi = 1$, and triangulation, we changed the position of each vertex by an amount $0 < \eta < 0.5$ at a random direction, and used the resulting distances as the reference lengths of each vertex. We then followed the regular procedure by stretching the strip, and letting the system relax (with the reference lengths calculated just a moment before).

Calculation through eq.(20)

A square patch was generated, independently of the simulation. Generation of the network itself was done similar to the way described in the simulation. However, once that calculated, instead of stretching the network we calculate $A^{\mu\nu\alpha\beta}$ using the $\{W_{(s)\lambda\tau}^{\mu\nu}\}$ which are calculated using eq.(20). Poisson's ratio is calculated in the mean field approximation as described in appendix B.

ACKNOWLEDGEMENTS

D.G would like to thank Amos Grossman for his help, patience and useful discussions, and to Alessio Zaccone for pointing out important references.

* doron.grossman@ladhyx.polytechnique.fr

- [1] S. Germain, *Recherches sur la théorie des surfaces élastiques* (V. Courcier, 1821).
- [2] A. L. B. Cauchy, *Exercices de mathématiques*, Vol. 1 (Chez De Bure Frères, 1826).
- [3] P. C. Martin, O. Parodi, and P. S. Pershan, Unified hydrodynamic theory for crystals, liquid crystals, and normal fluids, *Physical Review A* **6**, 2401 (1972).
- [4] F. Miserez, S. Ganguly, R. Haussmann, and M. Fuchs, Continuum mechanics of nonideal crystals: Microscopic approach based on projection-operator formalism, *Physical Review E* **106**, 054125 (2022).
- [5] A. Lemaître and C. Maloney, Sum rules for the quasi-static and visco-elastic response of disordered solids at zero temperature, *Journal of Statistical Physics* **123**, 415 (2006).
- [6] A. Zaccone, *Theory of Disordered Solids* (Springer International Publishing, 2023).
- [7] M. Schlegel, J. Brujic, E. M. Terentjev, and A. Zaccone, Local structure controls the nonaffine shear and bulk moduli of disordered solids, *Scientific Reports* **6**, 10.1038/srep18724 (2016).
- [8] B. Cui, G. Ruocco, and A. Zaccone, Theory of elastic constants of athermal amorphous solids with internal stresses, *Granular Matter* **21**, 10.1007/s10035-019-0916-4 (2019).
- [9] A. Zaccone and E. Scossa-Romano, Approximate analytical description of the nonaffine response of amorphous solids, *Physical Review B* **83**, 184205 (2011).
- [10] G. Gompper and D. M. Kroll, Random surface discretizations and the renormalization of the bending rigidity, *Journal de Physique I* **6**, 1305 (1996).
- [11] M. Kot, H. Nagahashi, and P. Szymczak, Elastic moduli of simple mass spring models, *The Visual Computer* **31**, 1339 (2014).
- [12] Y. Kantor and D. R. Nelson, Phase transitions in flexible polymeric surfaces, *Physical Review A* **36**, 4020 (1987).
- [13] H. S. Seung and D. R. Nelson, Defects in flexible membranes with crystalline order, *Physical Review A* **38**, 1005 (1988).
- [14] M. H. Bailey and M. Wilson, Self assembly of model polymers into biological random networks, *Computational and Structural Biotechnology Journal* **19**, 1253 (2021).
- [15] P. T. Underhill and P. S. Doyle, On the coarse-graining of polymers into bead-spring chains, *Journal of Non-Newtonian Fluid Mechanics* **122**, 3 (2004).
- [16] M. Moshe, M. J. Bowick, and M. C. Marchetti, Geometric frustration and solid-solid transitions in model 2d tissue, *Physical Review Letters* **120**, 268105 (2018).
- [17] M. Chen and F. J. Boyle, Investigation of membrane mechanics using spring networks: Application to red-blood-cell modelling, *Materials Science and Engineering: C* **43**, 506 (2014).
- [18] J. Bolander and S. Saito, Fracture analyses using spring networks with random geometry, *Engineering Fracture Mechanics* **61**, 569 (1998).
- [19] J. W. Rocks, N. Pashine, I. Bischofberger, C. P. Goodrich, A. J. Liu, and S. R. Nagel, Designing allostery-inspired response in mechanical networks, *Proceedings of the National Academy of Sciences* **114**, 2520 (2017).
- [20] J. Liu, Y. Nie, H. Tong, and N. Xu, Realizing negative poisson's ratio in spring networks with close-packed lattice geometries, *Physical Review Materials* **3**, 055607 (2019).
- [21] Y. Luo, C.-L. Ho, B. R. Helliker, and E. Katifori, Flow-network-controlled shape transformation of a thin membrane through differential fluid storage and surface expansion, *Physical Review E* **107**, 024419 (2023).
- [22] E. Efrati, E. Sharon, and R. Kupferman, Elastic theory of unconstrained non-euclidean plates, *Journal of the Mechanics and Physics of Solids* **57**, 762 (2009).
- [23] M. Zhang, D. Grossman, D. Danino, and E. Sharon, Shape and fluctuations of frustrated self-assembled nano ribbons, *Nature Communications* **10**, 10.1038/s41467-019-11473-6 (2019).
- [24] I. Levin, E. Siéfert, E. Sharon, and C. Maor, Hierarchy of geometrical frustration in elastic ribbons: Shape-transitions and energy scaling obtained from a general asymptotic theory, *Journal of the Mechanics and Physics of Solids* **156**, 104579 (2021).

- [25] E. Efrati, E. Sharon, and R. Kupferman, The metric description of elasticity in residually stressed soft materials, *Soft Matter* **9**, 8187 (2013).
- [26] L. J. Gibson, M. F. Ashby, G. S. Schajer, and C. I. Robertson, The mechanics of two-dimensional cellular materials, *Proceedings of the Royal Society of London. A. Mathematical and Physical Sciences* **382**, 25 (1982).
- [27] M. Tsamados, A. Tanguy, C. Goldenberg, and J.-L. Barrat, Local elasticity map and plasticity in a model lennard-jones glass, *Physical Review E* **80**, 026112 (2009).

Supplemental Material

Appendix A: Multi - index notation

Here we write explicitly the expressions of the multi-index notation of the matrices $A^{SS'}$ and $B^{SS'}$ that appear in the text. One way to directly build them is to first write the matrices W in terms of their independent terms (labeled W_n) and similarly for the matrix A . Then calculate the multiplication $M^{\mu\nu\alpha\beta} = A^{\mu\nu\rho\sigma}W_{\rho\sigma}^{\alpha\beta}$. At this point we vectorize W , and use the same scheme to vectorize M (which has the same number of independent components as W), and δA . We now define $A^{LL'} = \frac{\partial M_L}{\partial W_{L'}}$.

E.g. in 2D - marking

$$A_s^{IJ} = \begin{pmatrix} A_s^{1111} & A_s^{1112} & A_s^{1211} & A_s^{1212} \\ A_s^{1121} & A_s^{1122} & A_s^{1221} & A_s^{1222} \\ A_s^{2111} & A_s^{2112} & A_s^{2211} & A_s^{2212} \\ A_s^{2121} & A_s^{2122} & A_s^{2221} & A_s^{2222} \end{pmatrix} = \begin{pmatrix} A_s^1 & A_s^2 & A_s^2 & A_s^3 \\ A_s^2 & A_s^3 & A_s^3 & A_s^4 \\ A_s^2 & A_s^3 & A_s^3 & A_s^4 \\ A_s^3 & A_s^4 & A_s^4 & A_s^5 \end{pmatrix} \quad (25)$$

$$W_s^{IJ} = \begin{pmatrix} W_{(s)11}^{11} & W_{(s)12}^{11} & W_{(s)11}^{12} & W_{(s)12}^{12} \\ W_{(s)21}^{11} & W_{(s)22}^{11} & W_{(s)21}^{12} & W_{(s)22}^{12} \\ W_{(s)11}^{21} & W_{(s)12}^{21} & W_{(s)11}^{22} & W_{(s)12}^{22} \\ W_{(s)21}^{21} & W_{(s)22}^{21} & W_{(s)21}^{22} & W_{(s)22}^{22} \end{pmatrix} = \begin{pmatrix} W_s^1 & W_s^2 & W_s^4 & W_s^5 \\ W_s^2 & W_s^3 & W_s^5 & W_s^6 \\ W_s^4 & W_s^5 & W_s^7 & W_s^8 \\ W_s^5 & W_s^6 & W_s^8 & W_s^9 \end{pmatrix} \quad (26)$$

Where repeating markings indicate that these elements are equal. Additionally the numbering of the W_s matrix elements suggest a possible vectorization scheme (which is used in this text).

It now follows by direct calculation that after vectorization

$$A_s^{LL'} = \begin{pmatrix} A_s^1 & 0 & 0 & 2A_s^2 & 0 & 0 & A_s^3 & 0 & 0 \\ 0 & A_s^1 & 0 & 0 & 2A_s^2 & 0 & 0 & A_s^3 & 0 \\ 0 & 0 & A_s^1 & 0 & 0 & 2A_s^2 & 0 & 0 & A_s^3 \\ A_s^2 & 0 & 0 & 2A_s^3 & 0 & 0 & A_s^4 & 0 & 0 \\ 0 & A_s^2 & 0 & 0 & 2A_s^3 & 0 & 0 & A_s^4 & 0 \\ 0 & 0 & A_s^2 & 0 & 0 & 2A_s^3 & 0 & 0 & A_s^4 \\ A_s^3 & 0 & 0 & 2A_s^4 & 0 & 0 & A_s^5 & 0 & 0 \\ 0 & A_s^3 & 0 & 0 & 2A_s^4 & 0 & 0 & A_s^5 & 0 \\ 0 & 0 & A_s^3 & 0 & 0 & 2A_s^4 & 0 & 0 & A_s^5 \end{pmatrix} \quad (27)$$

$\delta A_s^{LL'}$ has the exact same structure, but with δA_s^n rather than A_s^n . We can now finally define $A^{SS'}$ and $B^{SS'}$ (independently of dimension)-

$$A^{SS'} = \left[\text{diag}_n(A_s^{LL'}) \right]^{S,S} = \begin{pmatrix} A_1^{LL'} & 0 & 0 & \\ 0 & A_2^{LL'} & 0 & \dots \\ 0 & 0 & A_3^{LL'} & \\ & \vdots & & \ddots \end{pmatrix} \quad (28)$$

$$B^{SS'} = \frac{1}{n} \left[\delta A_s^{LL'} \otimes \text{ones}_n \right]^{S,S} = \frac{1}{n} \begin{pmatrix} \delta A_1^{LL'} & \delta A_2^{LL'} & \delta A_3^{LL'} & \\ \delta A_1^{LL'} & \delta A_2^{LL'} & \delta A_3^{LL'} & \dots \\ \delta A_1^{LL'} & \delta A_2^{LL'} & \delta A_3^{LL'} & \\ & \vdots & & \ddots \end{pmatrix} \quad (29)$$

In three dimensions the same logic follows. The matrices look different, as they are much larger.

Appendix B: Mean field approximation

Within a geometric mean field, \mathbf{g} is assumed constant in space. We begin by considering one edge lies at coordinate $y = 0$, the other one at coordinate $y = y_m$, and similarly there are edges at $x = 0$ and $x = x_m$. At time zero we deform the network in real space $\vec{R} = \{X(x, y), Y(x, y)\}$ so that $|Y(y = y_m) - Y(y = 0)| = L$. We take this constraint into

account by introducing an effective energy using a Lagrange multiplier λ which is the stress on the boundary causing the stretching of the tissue.

$$\begin{aligned} E_{ext} &= \int \lambda \left(\left| \vec{R}(y = y_m) - \vec{R}(y = 0) \right| - L \right) dx = \int dx \lambda \left(\left| \int_0^{y_m} \partial_y \vec{R} dy \right| - L \right) dx \\ &= \int \lambda \left(\sqrt{\int \int \vec{R}'(y) \cdot \vec{R}'(y') dy' dy} - L \right) dx. \end{aligned} \quad (30)$$

Within the mean field approximation, $\vec{R}'(y) = \partial_y \vec{R}(y) = \text{const}$. So that $\vec{R}'(y) \cdot \vec{R}'(y') = g_{22}$ we can write

$$\begin{aligned} E_{ext} &= \int \lambda \left(\sqrt{y_m^2 g_{22}} - L \right) dx = \int \lambda \left(y_m \sqrt{g_{22}} - y_m \sqrt{G} \right) dx = \int \lambda y_m \left(\sqrt{g_{22}} - \sqrt{G} \right) dx \\ &= \int \lambda \left(\sqrt{g_{22}} - \sqrt{G} \right) dy dx \end{aligned} \quad (31)$$

where the length scale of the stretched network is $L = \sqrt{G} y_m$.

Taking the variation of the total energy $E = E_{el} + E_{ext}$, where is $E_{el} = \int \|\mathbf{g} - \bar{\mathbf{g}}\|^2 dV$ is the elastic energy (and $\bar{g}_{\mu\nu} = \delta_{\mu\nu}$) with respect to g and λ we derive the following equations:

$$\begin{aligned} \sqrt{g_{22}} - \sqrt{G} &= 0 \\ \sigma^{\mu\nu} &= \sigma_{el}^{\mu\nu} + \frac{\lambda}{2\sqrt{g_{22}}} \begin{pmatrix} 0 & 0 \\ 0 & 1 \end{pmatrix} \end{aligned} \quad (32)$$

where $\sigma_{el}^{\mu\nu}$ is the elastic stress. In principle, in order to find the metric $g_{\mu\nu}$ minimizing the elastic energy we must find the stress so that on the boundaries $y = 0$ and $y = y_m$, the stress balances the force. In the mean field approximation the conditions at the boundary impose $\sigma^{\mu\nu} = 0$. Using $G = 1 + \epsilon$ we get the required expression.

Appendix C: Ordered networks

In an ordered network, calculation is fairly simple. As $\tilde{A}^{\mu\nu\alpha\beta} = A^{\mu\nu\alpha\beta} = A_s^{\mu\nu\alpha\beta}$ is uniform and the non-affine coefficients are 0. Where, with a little abuse of notation

$$A^{\mu\nu\alpha\beta}(x) = \langle A^{\mu\nu\alpha\beta} \rangle = \frac{1}{N_s(\Omega)} \sum_{s \in \Omega(x)} A_{(s)}^{\mu\nu\alpha\beta} = \frac{1}{N_s(\Omega)} \sum_{s \in \Omega(x)} \sum_{e \in s} \frac{k_e \Delta x_e^\mu \Delta x_e^\nu \Delta x_e^\alpha \Delta x_e^\beta}{16 \ell_e^2},$$

and $\Omega(x)$ is some region around the point, x .

For an ordered systems, it is enough to consider just a small, finite sum of a few simplex edges (in two dimension these are just triangles). We used $k_e = 1$, and thus $A^{\mu\nu\alpha\beta} = \ell_1^2 (\cos \theta_1)^a (\sin \theta_1)^b + \ell_2^2 (\cos \theta_2)^a (\sin \theta_2)^b + \ell_3^2 (\cos \theta_3)^a (\sin \theta_3)^b$, where $a = 8 - \mu - \nu - \alpha - \beta$, $b = 4 - a$, ℓ_1, ℓ_2, ℓ_3 are the reference lengths of the edges, $\theta_1, \theta_2, \theta_3$ are the angles of the edges relative to the "1" direction, and $\mu, \nu, \alpha, \beta \in (1, 2)$. We thus solve for $g_{11} - 1 = -\nu(g_{22} - 1)$.

We modeled each triangle as composed of the following vertexes (up to a global rotation angle Θ of the triangles relative to the stretching direction)

$$\{(0, 0), (\phi/2, \psi\sqrt{3})/2, (0, 1)\}$$

ϕ corresponds to "shearing" of the lattice unit cell, while ψ corresponds to "elongation". This results with the edge list

$$\{(0, 1), (\phi/2, \psi\sqrt{3}/2), (1 - \phi/2, -\psi\sqrt{3}/2)\}$$

and the reference lengths $\{1, \sqrt{\phi^2 + 3\psi^2}/2, \sqrt{(1 - \phi)^2 + 3\psi^2}/2\}$

The theoretical calculation results with a complicated expression that can be evaluated

$$\nu = - \frac{P(\phi, \psi, \Theta)}{4Q(\phi, \psi, \Theta)} \quad (33)$$

$$\begin{aligned} P(\phi, \psi, \Theta) &= \cos(4\theta) \{ 27\psi^6 - (\phi - 2)^2 \phi^2 [\phi^2 - 2\phi + 4] + 9\psi^4 (\phi^2 - 2\phi) - 3\psi^2 [(\phi^2 - 2\phi)(\phi^2 - 2\phi - 20) - 16] \} \\ &\quad + \sin(4\theta) \left\{ 2\sqrt{3}\psi(\phi - 1) [9\psi^4 + 6\psi^2(\phi^2 - 2\phi - 2) + (\phi^2 - 2\phi)(\phi^2 - 2\phi + 8)] \right\} - 48\psi^2 \\ &\quad + (\phi^2 - 2\phi - 3\psi^2) [9\psi^4 + 6\psi^2(\phi^2 - 2\phi) + (\phi^2 - 2\phi)(\phi^2 - 2\phi + 4)] \\ Q(\phi, \psi, \Theta) &= 36\psi^4 \sin^4(\theta) + 2 \cos^4(\theta) [6\psi^2(\phi^2 - 2\phi)^2 + (\phi^2 - 2\phi)^2(\phi^2 - 2\phi + 4) + 9\psi^4(\phi^2 - 2\phi + 2)] \\ &\quad + 6\psi^2 \sin^2(\theta) \cos^2(\theta) (9\psi^4 + \phi^4) + 3\psi^2 \sin^2(2\theta) [3\psi^2(\phi^2 - 2\phi + 2) - 2(\phi - 2)(\phi^2 - 4\phi + 2)] \\ &\quad - 4\sqrt{3}\psi(\phi - 1) \sin(\theta) \cos^3(\theta) (9\psi^4 + 6\psi^2(\phi^2 - 2\phi) + (\phi^2 - 2\phi)(\phi^2 - 2\phi + 8)) - 48\sqrt{3}\psi^3(\phi - 1) \sin^3(\theta) \cos(\theta). \end{aligned}$$

For each ϕ ψ values the results are then plotted as a function of Θ and are compared to simulation.